



Impact of linewidth enhancement factor and gain suppression on chirp characteristics of high-speed laser diode and performance of 40 Gbps optical fiber links

Nada Fouad¹ · Tarek Mohamed¹ · Alaa Mahmoud¹

Received: 21 October 2021 / Accepted: 26 January 2022 / Published online: 12 February 2022
© The Author(s) 2022

Abstract

We present a simulation study on the chirping characteristics of a directly modulated 40 Gbps laser diode and evaluate its performance for use in high-speed optical fiber links. The effects of the linewidth enhancement factor (α) and gain suppression on the laser chirp and the maximum fiber transmission length are investigated. The chirp characteristics include the frequency peak-to-peak chirp of the time-varying frequency and shift of the emission wavelength. The performance of 40 Gbps optical fiber link is evaluated in terms of the eye diagram and quality factor of the received signal, which helps in predicting the maximum fiber length that achieves error-free transmission. The results show that when α increases from 1 to 10, the overshoots of the relaxation oscillations become strong, resulting in a sharp increase in laser peak-to-peak chirp from 21.8 to 205 GHz. The increase of gain suppression factor from $\epsilon = 0.5 \times 10^{-17} \text{ cm}^3$ to $\epsilon = 5 \times 10^{-17} \text{ cm}^3$ dampens out the overshoots and slightly reduces the peak-to-peak chirp from 19.5 to 193.3 GHz. Although the gain suppression works to reduce the laser chirp, it causes a significant wavelength shift relative to the emission wavelength of the non-modulated laser, which degrades the efficiency of the laser diode. On the other hand, the gain suppression is shown to increase the degree of eye-opening and the corresponding Q -factor of the fiber link on a reverse action of the linewidth enhancement factor. As fiber length increases, the influences of α and ϵ on chirp characteristics become more significant. The maximum fiber length (L_{\max}) is shown to decrease with the increase in α and/or ϵ ; when α increases from 1 to 10, L_{\max} decreases from 5.89 to 0.78 km at $\epsilon = 5 \times 10^{-17} \text{ cm}^3$, and decreases from 2.52 to 0.3 km at $\epsilon = 0.5 \times 10^{-17} \text{ cm}^3$.

1 Introduction

With the developments in high-speed optical networks, 40 Gbps optical transmission systems have received a considerable interest for use in very-short-reach optical links [1]. Laser diodes (LDs) are widely used as light sources in optical transmission systems. The laser signal is modulated with an electrical signal through either direct or external modulation [2]. In the direct modulation, the electrical signal (information signal) is applied directly to the LD in conjunction with the bias current. This simple implementation gives several advantages such as low cost and low power consumption when compared to external modulation [2, 3]. However, direct intensity modulation of LDs resulting

in a simultaneous phase modulation through the linewidth enhancement factor (α -factor) [4], which causes a time variation in the lasing frequency (i.e., frequency modulation) [5]. The interdependence between intensity and frequency modulation is referred to as “frequency chirp” [2]. In digital transmission systems, high-speed lasers that meet the requirement of 40 Gbps short-reach data communication links usually have a large differential gain, which increase the frequency chirp [6, 7]. The frequency chirp typically causes variations in the pulse width, which when combined with fiber dispersion degrades the digital system performance [7–11]. This degradation imposes limitations on the transmission bit rate and transmission distance [12, 13]. Another serious limitation of frequency chirp is that it causes shifting in the emission wavelength of the laser, which is a critical issue in applications like wavelength division multiplexing (WDM) systems to avoid channel interference [14]. The chirping behavior of directly modulated LDs is characterized by two chirp types: transient and adiabatic chirp, which are influenced by laser design parameters and operating conditions

✉ Alaa Mahmoud
alaa.abutaleb@lira.bsu.edu.eg

¹ Laser Institute for Research and Applications LIRA, Beni-Suef University, Beni-Suef 62511, Egypt

[15]. The transient chirp appears around the rise/fall locations of the pulse and originates from the turn-on relaxation oscillations. These relaxation oscillations occur as a result of electron–photon coupling through stimulated emission during the transition between steady states [16]. On the other hand, the adiabatic chirp is the frequency offset induced between laser steady-state output powers (around the mean values in both “1” and “0” levels) [15]. The transient chirp causes variations in pulse width, whereas the adiabatic chirp induces a shift in the emission wavelength [14].

The laser design and structure parameters that control these types of frequency chirp are the linewidth enhancement factor (α -factor) [17, 18] and gain suppression [19–21]. The α -factor describes the refractive index variations with the injected carrier density and its impact on the dynamical properties of the LDs [22, 23]. The changes in the injected carrier density induces simultaneous changes in the optical gain and refractive index of the active region, resulting in an intensity–phase coupling, which increases the laser linewidth by a factor of $1 + \alpha^2$ [17, 18, 24]. On the other hand, the effect of gain suppression is to prevent the carrier density above the threshold value from getting tightly clamped, resulting in a reduction in the optical gain by the factor of $(1 + \epsilon S)^{-1}$ at high photon densities (S) [21]. The gain suppression suppresses the carrier–photon resonance and increases the damping rate of relaxation oscillations, which then reduces the transient chirp and introduces adiabatic chirp [20, 25]. The gain suppression was attributed to many physical mechanisms, including intraband relaxation processes of injected carriers [26], spectral hole burning [27], nonlinear absorption [28], carrier diffusion [29], and dynamic carrier heating effects [30].

It is beneficial to investigate the effect of these important laser parameters on the chirp characteristics induced by directly modulated LDs, especially at high modulation bit rates. The previous studies [31, 32] reported that the increase in ϵ increases the adiabatic chirp, and reduces the transient chirp at modulation bit rates of 5 and 10 Gbps. However, the findings reported in Ref. [33] revealed that the gain suppression causes enhancement in the modulated signal quality at 2 and 10 Gbps. On the other hand, it was reported in Ref. [14] that at 10 Gbps modulation, the adiabatic chirp is the main contributor to degradation of directly modulated WDM systems. In addition, the authors in Ref. [34] confirmed that in directly modulated WDM systems, frequency chirp reduces the transmission bit rate and vice versa at long fiber lengths. In comparison to the 10 Gbps modulation, Ref. [6] showed experimentally and theoretically that at a high modulation bit rate of 40 Gbps, the adiabatic chirp is undistinguishable and the transient chirp is dominating. Regardless of the chirp type, it was reported that at high-speed modulation, the laser chirp is combined with the fiber dispersion in such a way to limit the fiber length [35, 36]. Although most of

previous studies focused on the impact of laser chirp on the system performance, there is still room for more in-depth investigation into impacts of both α -factor and ϵ on the frequency chirp and the maximum fiber length, especially at a high modulation bit rate of 40-Gbps. In addition, there is a lack of studies on the influence of these parameters on the emission shifting associated with digital modulation of the laser, which is a critical issue in WDM system performance avoiding the channel interference [14, 22, 37].

In this paper, we present intensive numerical simulations on the effects of the α -factor and gain suppression coefficient on the chirp characteristics of a directly modulated high-speed 1.55 μm laser diode and evaluate its performance for use in 40 Gbps optical fiber links. The chirp characteristics include the modulated signal waveform, frequency peak-to-peak chirp, and shift of the emission wavelength. The performance of 40 Gbps optical fiber link is evaluated in terms of eye diagram and Q -factor of the received laser signal, and estimation of the maximum fiber transmission length. The simulated study is based on the rate equation model of laser diode subject to digital non-return to zero (NRZ) pseudo-random bit format using the “Optisystem” software.

The theoretical model and simulation method used in this study is given in Sect. 2. The simulation results and discussion are presented in Sect. 3, and the conclusions appear in Sect. 4.

2 Theoretical model and simulation method

The dynamic behavior and modulation characteristics of a single-mode LD are typically modeled by numerical integrating the following coupled rate equations using the fourth-order Runge–Kutta algorithm. These rate equations describe the time evolution of the injected carrier density $N(t)$ into the active layer, emitted photon density $S(t)$ and optical phase $\phi(t)$ [38].

$$\frac{dN(t)}{dt} = \frac{I(t)}{eV} - \frac{N(t)}{\tau_c} - \frac{g_o(N(t) - N_o)}{1 + \epsilon S(t)} S(t) \quad (1)$$

$$\frac{dS(t)}{dt} = \frac{\Gamma g_o(N(t) - N_o)}{1 + \epsilon S(t)} S(t) - \frac{S(t)}{\tau_p} + \frac{\Gamma \beta N(t)}{\tau_c} \quad (2)$$

$$\frac{d\phi(t)}{dt} = \frac{\alpha}{2} \left[\Gamma g_o(N(t) - N_o) - \frac{1}{\tau_p} \right], \quad (3)$$

where $I(t)$ is the waveform of the injection current, V is the volume of the active region, e is the electron charge, τ_c is the electron lifetime, ϵ is the nonlinear gain suppression coefficient, $g_o = v_g a_o$ is the gain slope constant with v_g being the group velocity and a_o the differential gain coefficient, N_o is

the carrier density required to achieve transparency, τ_p is the photon lifetime, Γ is the optical confinement factor and β is the spontaneous emission factor. It is worth noting that the gain suppression coefficient ε was added phenomenologically to the nonlinear gain form in Eqs. (1) and (2) to describe the nonlinear photon density dependence of optical gain (i.e. the optical gain saturates at high photon densities) [39]. This phenomenological addition of ε prevents the carrier density above the threshold value from getting tightly clamped, inducing a reduction in the optical gain by the factor of $(1 + \varepsilon S)^{-1}$ at high photon densities [21]. While another phenomenological form for gain nonlinearity of $g_o(N - N_o)$ ($1 - \varepsilon S$) is frequently used [11, 40], a gain formula was derived basing on a perturbation approach along with density matrix analysis and fitting the theoretical results as $g_o(N - N_o) - BS$, B being a nonlinear gain coefficient [26]. According to [41], at high photon densities, the nonlinear gain form in Eqs. (1) and (2) agrees best with numerical solutions, while the gain form of $g_o(N - N_o)(1 - \varepsilon S)$ tends to fail. However, the differences in the laser dynamics, for example the resonance frequency, damping rate and noise, simulated by all these nonlinear gain formulas are very small especially within the normal range of injection current of the LDs [42].

The direct modulation of LDs is described by representing the injection current of Eq. (1) as

$$I(t) = I_b + I_{in}(t)I_m, \quad (4)$$

where I_b is the bias current, I_m is the modulation current and $I_{in}(t)$ is the form of the input signal (either “0” or “1” in digital modulation). The time variation of the modulated laser output power $P(t)$ is determined from the photon density $S(t)$ via the relationship:

$$P(t) = \frac{V\eta_o h\nu}{2\Gamma\tau_p} S(t), \quad (5)$$

where η_o is the differential quantum efficiency, ν is the optical frequency, and h is the Planck’s constant. The time-dependent optical frequency variation (chirp) within the active region of a directly large signal modulation of single-mode LD can be obtained from the phase rate equation as

$$\Delta\nu(t) = \frac{1}{2\pi} \left(\frac{d\phi}{dt} \right). \quad (6)$$

Using Eqs. (1)–(5), the frequency chirp can be obtained in terms of the modulated laser output optical power as [11, 43, 44]:

$$\Delta\nu(t) = \frac{\alpha}{4\pi} \left\{ \frac{d}{dt} [\ln P(t)] + kP(t) \right\}, \quad (7)$$

where α is the linewidth enhancement factor and k is the adiabatic chirp coefficient. The α -factor quantifies the variations of the refractive index and gain with the carrier density N inside the cavity, and describes their effect on the dynamical properties of LD using the following equation [17]:

$$\alpha = -\frac{4\pi}{\lambda} \left(\frac{\partial n / \partial N}{\partial g / \partial N} \right), \quad (8)$$

where n is the refractive index, g is the gain per unit length and λ is the wavelength. Whereas, the adiabatic chirp coefficient k depends on the laser structure and is directly related to the nonlinear gain suppression coefficient ε through the following expression [11]:

$$k = \frac{2\Gamma}{V\eta_o h\nu} \varepsilon. \quad (9)$$

The chirp from the first term of Eq. (7) corresponds to the transient chirp and it has a significant value during the relaxation oscillations of the laser. This indicates that devices with strong damping relaxation oscillations exhibit good transient chirp characteristics resulting from the reduction in the rate of change of $\ln P(t)$. The second term of Eq. (7) corresponds to the adiabatic chirp, which arises from spontaneous emission and nonlinear gain suppression effects, and is associated with the frequency offset between the “1” and “0” power levels during the modulation.

The proposed simulation setup of the optical fiber communication link used in this study is schematically shown in Fig. 1. The data sequence (information code) at bit rate of 40 Gbps is generated by pseudo-random bit sequence (PRBS) generator with bit-sequence length of $2^7 - 1 = 127$ bits, which is the term of $I_{in}(t)$ in Eq. (4). The NRZ pulse generator then converts this information code into an electrical signal as square pulses with NRZ format. Direct modulation of the laser diode is performed by injecting the modulation current I_m (shaped with the NRZ bit format) directly in conjunction with bias current I_b . The time variations of the modulated laser output power $P(t)$ and the corresponding frequency chirp $\Delta\nu$ are observed by the optical time domain visualizer. The wavelength spectrum of the optical power is recorded by the optical spectrum analyzer. The modulated laser signal is then transmitted down a standard single-mode fiber (SSMF) with attenuation coefficient $\alpha_f = 0.2$ dB km⁻¹ and dispersion $D = 16.75$ ps/(nm km). The received laser signal is detected and converted into an electrical signal by a PIN photodetector of responsivity = 1 A/W and dark current = 10 nA, which is used in conjunction with low-pass Bessel filter of order four [41]. The transmission quality of the modulated signal is characterized in terms of the eye diagram and the associated Q -factor of the received laser signal, which are recorded by the eye diagram analyzer. The calculated Q -factor is defined as [45]:

Fig. 1 The proposed simulation setup of direct modulation of laser diode system used in the study

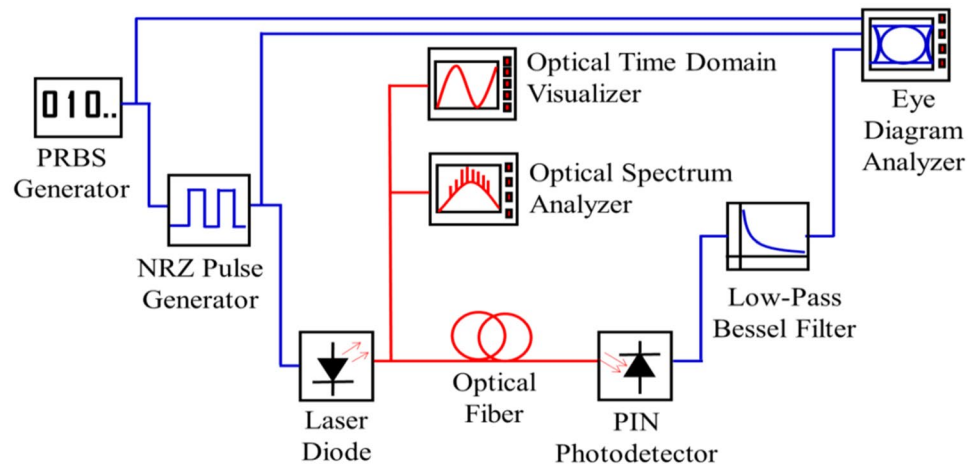


Table 1 The parametric values of the laser diode used in the proposed high-speed fiber communication link [6]

Parameter	Symbol	Value
Wavelength	λ	1.55 μm
Active layer volume	V	$3 \times 10^{-11} \text{ cm}^3$
Group velocity	v_g	$8.33 \times 10^9 \text{ cm/s}$
Quantum efficiency	η_0	0.255
Differential gain coefficient	a_0	$9.9 \times 10^{-16} \text{ cm}^2$
Carrier density at transparency	N_o	$1.23 \times 10^{18} \text{ cm}^{-3}$
Linewidth enhancement factor	α	(1-10)
Mode confinement factor	Γ	0.2
Photon lifetime	τ_p	$1.69 \times 10^{-12} \text{ s}$
Electron lifetime	τ_c	$776 \times 10^{-12} \text{ s}$
Spontaneous emission factor	β	3×10^{-5}
Gain suppression coefficient	ϵ	$(0.5-5) \times 10^{-17} \text{ cm}^3$
Threshold current	I_{th}	9.8 mA
Bias current	I_b	92 mA
Modulation current	I_m	90 mA

$$Q = \frac{|\mu_1 - \mu_0|}{\sigma_1 + \sigma_0}, \quad (10)$$

where μ_j and σ_j with $j = "1"$ or $"0"$, are the average values and standard deviations of the sampled values, respectively. The greater the difference between the average signal levels for a "1" and a "0", the more eye-opening and the higher the Q -factor, and thus the lower the bit error rate (BER). According to ITU-T recommendations, BER is limited by 10^{-12} , which corresponds to $Q \approx 7$.

The parameters and the corresponding numerical values of the laser diode used in the calculations are listed in Table 1 [6]. The proposed laser diode is InGaAsP-DFB laser diode radiating in wavelength of 1.55 μm [6].

3 Results and discussion

3.1 Laser signal and chirp characteristics

The influences of the linewidth enhancement factor α and gain suppression coefficient ϵ on the time variation characteristics of the modulated laser signal power (on the left-hand axis) and associated frequency chirp (on the right-hand axis) at a high bit rate B of 40 Gbps are illustrated in Fig. 2a–d. The figures investigate four study cases: (1) small values of α and ϵ as shown in Fig. 2a, (2) small α and large ϵ as shown in Fig. 2b, (3) large α and small ϵ as shown in Fig. 2c, and (4) large values of α and ϵ as shown in Fig. 2d. Figure 2a shows that when the laser has small $\alpha = 1$ and small $\epsilon = 0.5 \times 10^{-17} \text{ cm}^3$, the modulated laser signal power exhibits pronounced relaxation oscillations (multiple peaks with different heights) in either the "1" or "0" levels that follow opposite levels. The rise and fall positions of the modulated laser signal result in blue and red shifts in frequency forming transient chirp of 21.8 GHz. The contribution for the adiabatic chirp almost does not exist in this case due to the small value of ϵ , where the difference between the "1" and "0" levels is very small. As a result, the transient chirp represents the peak-to-peak chirp. The influence of ϵ appears in Fig. 2b when it has a large value of $5 \times 10^{-17} \text{ cm}^3$ and α remains as small as 1. The increase in ϵ causes a significant difference between the "1" and "0" levels, inducing a pronounced adiabatic chirp of 14.9 GHz as seen in the right-hand axis of Fig. 2b. In addition, the increase in ϵ strengthens the damping rate of laser relaxation oscillations, shrinking the time instants at which the oscillations die away and decreasing the peak overshoot of the oscillations due to the decrease in the photon density $S(t)$ inside the cavity [32, 46]. This is consistent with the findings reported in Refs. [33, 46–48]. Although the adiabatic chirp contributes significantly at large ϵ , the strengthening of the damping rate and the associated decrease in the peak overshoot of the

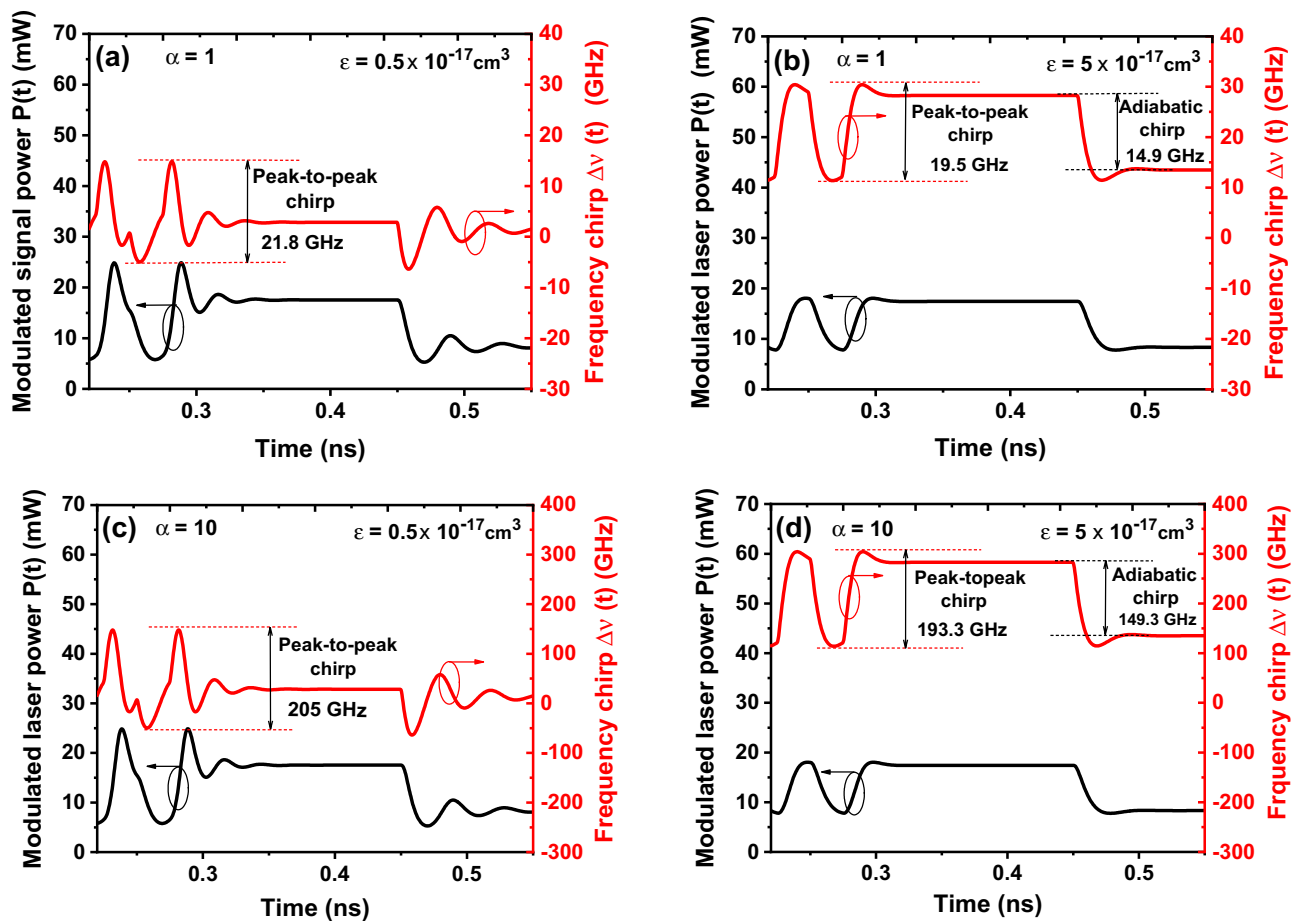


Fig. 2 Simulated time variation characteristics of the modulated laser power (on the left hand axis) and the associated frequency chirp (on the right hand axis) at 40 Gbps NRZ modulation when **a** $\alpha = 1$

and $\epsilon = 0.5 \times 10^{-17} \text{ cm}^3$, **b** $\alpha = 1$ and $\epsilon = 5 \times 10^{-17} \text{ cm}^3$, **c** $\alpha = 10$ and $\epsilon = 0.5 \times 10^{-17} \text{ cm}^3$, and **d** $\alpha = 10$ and $\epsilon = 5 \times 10^{-17} \text{ cm}^3$

relaxation oscillations work to reduce the transient chirp, which in turn reduces the peak-to-peak chirp to 19.5 GHz when compared with the value of first case (21.8 GHz). Figure 2c investigates the effect of α -factor when it is set to be as large as 10 at small ϵ value of $0.5 \times 10^{-17} \text{ cm}^3$ (the third case). The figure shows that the large value of α causes stronger overshooting of the laser relaxation oscillation, which induces a high contribution to the transient chirp in agreement with interpretations reported in Ref. [37]. This high contribution of the transient chirp increases the peak-to-peak chirp significantly that reaches 205 GHz. Modulating the laser with large values of ϵ ($= 5 \times 10^{-17} \text{ cm}^3$) and α ($= 10$) is illustrated in Fig. 2d, which represent the fourth case. The figure reveals that the adiabatic chirp rises to 149.3 GHz (as compared to Fig. 2b), while the peak-to-peak chirp reduces to 193.3 GHz (as compared to Fig. 2c). The above results indicate that the adiabatic chirp results from the gain suppression effect, whereas the transient chirp is associated with the large α -factor. Also, the laser peak-to-peak chirp reduces (i.e., improves the chirp characteristics)

as the α -factor decreases and/or ϵ increases, although the increase in ϵ enhances the adiabatic chirp.

Figure 3 plots variations of the laser peak-to-peak chirp at a high bit rate of 40 Gbps as a function of the α -factor at two gain suppression coefficients of $\epsilon = 0.5 \times 10^{-17}$ and $5 \times 10^{-17} \text{ cm}^3$. The figure reveals that the laser peak-to-peak chirp is significantly influenced by the α -factor, whereas it is slightly influenced by the gain suppression coefficient ϵ . The laser peak-to-peak chirp increases sharply as the α -factor increases from 1 to 10, while it is slightly reduced as ϵ increases from 0.5×10^{-17} to $5 \times 10^{-17} \text{ cm}^3$. This reduction becomes more significant when the α -factor increases; when ϵ increases from 0.5×10^{-17} to $5 \times 10^{-17} \text{ cm}^3$, the peak-to-peak chirp values differ by 2.3 GHz at $\alpha = 1$ (19.5 and 21.8 GHz), whereas they differ by 11.7 GHz at $\alpha = 10$ (193.3 and 205 GHz).

The influences of α -factor and gain suppression coefficient ϵ on the wavelength spectrum of the modulated laser signal power are illustrated in Fig. 4. The spectrum characteristics provide useful information on the wavelength shift

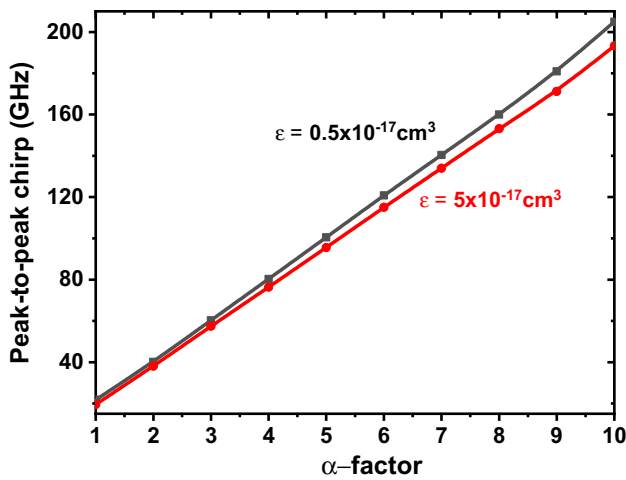


Fig. 3 Variations of the laser peak-to-peak chirp with the α -factor at small gain suppression coefficient ϵ of $0.5 \times 10^{-17} \text{ cm}^3$ (black line), and at large ϵ of $5 \times 10^{-17} \text{ cm}^3$ (red line)

($\Delta\lambda$) of the emission wavelength relative to the wavelength of the non-modulated laser. This wavelength shift is a primary cause to limitation of the WDM system performance [14, 22]. Figure 4a plots the wavelength spectrum of the modulated laser signal when the laser is simulated with the small value of $\alpha=1$ under two values of $\epsilon=0.5 \times 10^{-17}$ (small) and $5 \times 10^{-17} \text{ cm}^3$ (large). The figure shows that when ϵ is small, the chirp becomes predominantly transient and the emission peak is nearly centered at the actual wavelength of laser emission (the wavelength shift is very low as $\Delta\lambda=0.02 \text{ nm}$). Whereas when ϵ is large, the chirp becomes predominantly adiabatic, creating two separated peaks that correspond to bits “1” and “0”, as illustrated in the inset of Fig. 4a. The wavelength separation between these two peaks ($\delta\lambda_A$) is directly related to the adiabatic chirp value [37, 49],

which is as small as $\delta\lambda_A=0.036 \text{ nm}$ in this case. The figure also reveals that when ϵ is large ($=5 \times 10^{-17} \text{ cm}^3$), the “1” bit has a small wavelength shift of $\Delta\lambda=0.177 \text{ nm}$ toward the shorter wavelength side of the spectrum (blue shift) as a result of the low effect of transient chirp induced by the small value of α -factor ($=1$). Whereas when the α -factor increases to 10, the transient chirp has a significant impact on the spectra, resulting in pronounced wavelength variations, which manifest as asymmetry in the optical spectra, as shown in Fig. 4b. It can be inferred that when ϵ increases from 0.5×10^{-17} to $5 \times 10^{-17} \text{ cm}^3$, $\delta\lambda_A$ increases from 0.325 to 1.23 nm, and $\Delta\lambda$ increases from 0.212 to 2.28 nm, respectively. Such results indicate degradation in the efficiency of laser diode in WDM applications [22, 37]. It is worth noting that the distinct separation between the wavelength of the “1 s” and the “0 s” (i.e. the blue shift of “1 s” relative to “0 s”) is due to the fact that the “0 s” have non-zero power (i.e. the extinction ratio is low enough). This is attributed to the carrier splitting effect with a frequency shift, which is expressed as [49]:

$$\Delta v(\{0\}) \leftrightarrow \{1\}) = \frac{\alpha k}{4\pi} \Delta P(\{0\}) \leftrightarrow \{1\}). \quad (11)$$

The carrier splitting effect is much stronger when the adiabatic and/or transient chirp are both dominant, producing a plateau between the “1” and “0” wavelength positions. When comparing Fig. 4a, b, it is clear that increasing α from 1 to 10 increases the laser spectral width and causes pulse broadening and inter-symbol interference as well as significant increase in the lasing wavelength shift $\Delta\lambda$ toward the shorter wavelength side of the spectrum. These results agree with the findings given in Ref. [37]. The increase in the lasing wavelength shifts $\Delta\lambda$ when $\alpha=10$ is attributed to the high adiabatic wavelength separation $\delta\lambda_A$ between the “1”

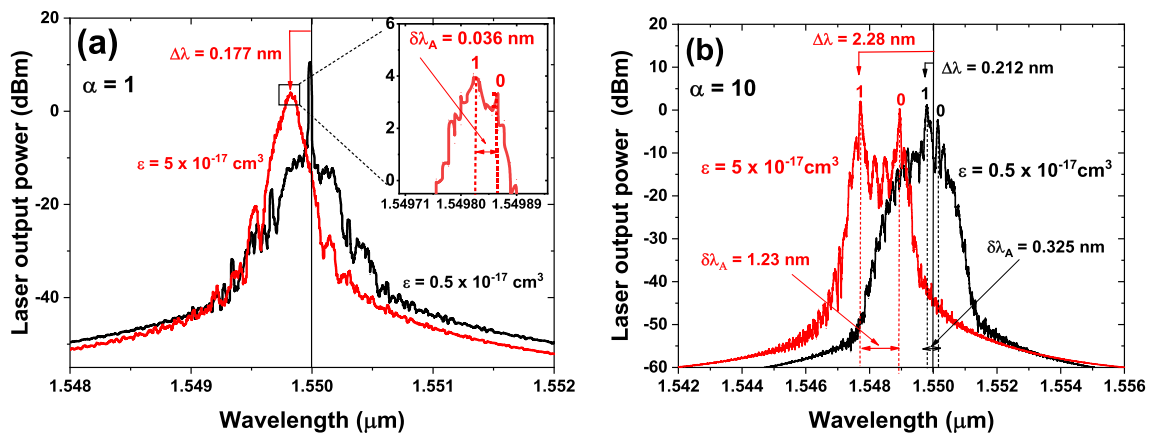


Fig. 4 Optical spectrum of the modulated laser signal output power when **a** $\alpha=1$ and **b** $\alpha=10$, at two different ϵ values of $0.5 \times 10^{-17} \text{ cm}^3$ (black lines) and $5 \times 10^{-17} \text{ cm}^3$ (red lines)

and “0” bits [37, 49]. These results agree with the experimental and theoretical findings reported in Ref. [49]. It can be concluded from the above results that although the gain suppression coefficient ϵ works to reduce the laser peak-to-peak chirp (i.e., improve the chirp characteristics) as shown in Fig. 3, it causes significant shifts in the lasing wavelength and degrades the efficiency of laser diode in WDM applications due to the channel interference [14].

Figure 5 demonstrates the variations of lasing wavelength shift $\Delta\lambda$ relative to the non-modulated laser wavelength as a function of the α -factor when the gain suppression coefficient ϵ is as small as $0.5 \times 10^{-17} \text{ cm}^3$ and as large as $5 \times 10^{-17} \text{ cm}^3$. The figure reveals that the wavelength shifts $\Delta\lambda$ increases when the α -factor and/or the ϵ increase; when α increases from 1 to 10, $\Delta\lambda$ increases from 0.02 to 0.212 nm when $\epsilon = 0.5 \times 10^{-17} \text{ cm}^3$, whereas it increases from 0.177 to 2.28 nm when $\epsilon = 5 \times 10^{-17} \text{ cm}^3$. The increase in $\Delta\lambda$ with the α -factor is slight when ϵ is small, whereas it becomes sharper when ϵ is large. This implies that the larger values of α and ϵ correspond to wider shift $\Delta\lambda$ for the emission wavelength relative to the actual non-modulated laser wavelength, which reduces the efficiency of the high-speed laser diode for use in WDM systems. The significant blue shift in the lasing wavelength $\Delta\lambda$ with the large ϵ value is explained as follows: the increase of ϵ works to increase the adiabatic chirp as mentioned above, which in turn increases the wavelength difference between the “1 s” and “0 s” that result from the carrier splitting effect [37, 49]. Moreover, the increase of ϵ enhances the effect of α -factor in the blue wavelength shifting that agrees with the results in Ref. [37] through the reduction of differential gain above threshold [32, 50]. These obtained results, to the best of the authors’

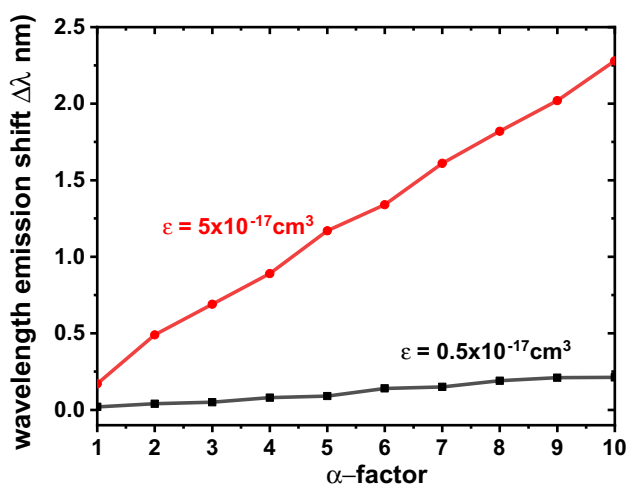


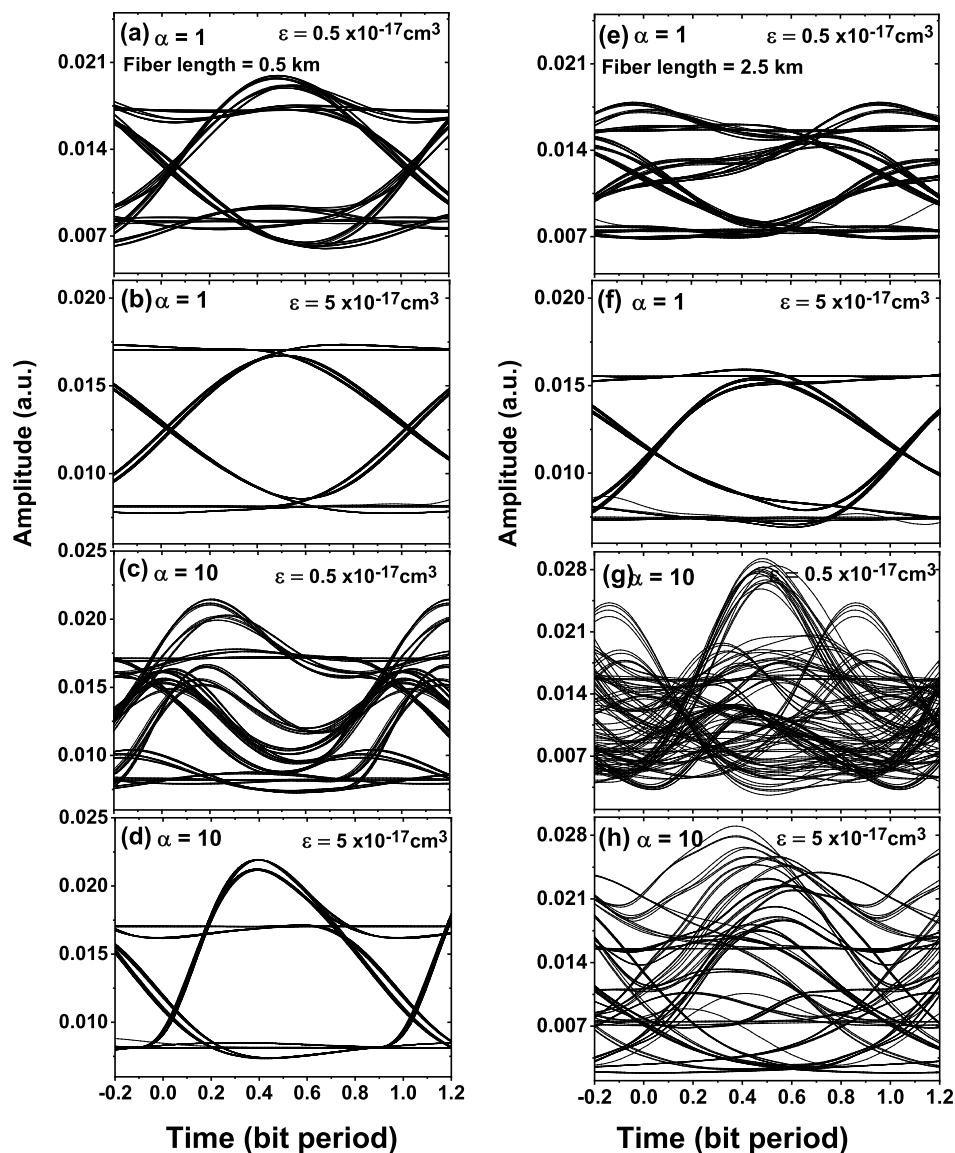
Fig. 5 Variations of the wavelength emission shift $\Delta\lambda$ relative to the actual non-modulated laser wavelength ($1.55 \mu\text{m}$) as a function of the α -factor at small gain suppression coefficient ϵ of $0.5 \times 10^{-17} \text{ cm}^3$ (black line), and at large ϵ of $5 \times 10^{-17} \text{ cm}^3$ (red line)

knowledge, represent new contributions to dependency of the lasing wavelength shifts on α and ϵ for 40-Gbps WDM systems.

3.2 Performance of the system quality

The performance of high-speed digital transmission systems is qualitatively evaluated using the eye diagram analysis of the laser waveform. This is a visual tool to examine the received laser signal quality by measuring the opening degrees of the eye diagram in both the vertical and horizontal directions [33]. The degree of vertical opening is estimated in terms of the Q -factor [45]. In the present simulations, the eye diagram is constructed by dividing the received laser signal waveform into two-bit segments and putting each onto others. The eye diagram analysis is used to investigate the effects of α and ϵ as well as the fiber length on the received signal quality in terms of the Q -factor at a high bit rate of 40 Gbps. Figure 6a–d demonstrates the evolution of the eye diagram under the four investigated cases of Fig. 2a–d, respectively, when the modulated signal is transmitted over a fiber of 0.5 km length, whereas Fig. 6e–h displays corresponding eye diagrams when the modulated signal is transmitted over 2.5 km fiber. Comparing the eye diagrams of Fig. 6a–d indicate that increasing ϵ from 0.5×10^{-17} to $5 \times 10^{-17} \text{ cm}^3$ works to enhance the degree of the eye-opening, improving the Q -factor from 8.48 (where eye diagram is partially closed) to 22.33 (where eye diagram is well opened) when $\alpha = 1$. On the other hand, when α is increased to 10, the increase in ϵ from 0.5×10^{-17} to $5 \times 10^{-17} \text{ cm}^3$ improves the Q -factor from 1.43 (completely closed eye diagram) to 16.17 (partially closed eye diagram). The increase of both the eye-opening and Q -factor with ϵ is attributed to increase in the damping rate of the relaxation oscillation (i.e., the level of the overshoot is damped out) in addition to reducing the random fluctuations in the turn-on delay time (time needed for the carrier density to reach the lasing threshold value), which then results in clear eye diagram [37]. The improvement of Q -factor with ϵ agrees with the findings given in Ref. [33]. In contrast, increasing the α -factor adds to the eye closure, which indicates deterioration in the modulated signal quality. When α increases from 1 to 10, the Q -factor decreases from 8.48 (the eye is partially closed) to 1.43 (the eye is completely closed) when $\epsilon = 0.5 \times 10^{-17} \text{ cm}^3$, and from 22.33 (the eye is well opened) to 16.17 (the eye is partially closed) when $\epsilon = 5 \times 10^{-17} \text{ cm}^3$. This reduction of the Q -factor with α is consistent with the results reported in Ref. [37]. The effects of α and ϵ on the chirp characteristics when including fiber nonlinearities are illustrated in Fig. 6e–h when the fiber length is increased to 2.5 km. Figure 6e–h reveals that there are significant reductions in Q -factors at 2.5 km fiber length when compared to those in Fig. 6a–d at 0.5 km fiber length, respectively.

Fig. 6 Eye diagram analysis at $B=40$ Gbps for the four investigated cases of Fig. 2a–d when the modulated signal transmitted over fiber with lengths of a–d 0.5 km, and e–h 2.5 km, respectively



As a numerical example, when the fiber length increases from 0.5 to 2.5 km, the Q -factor reduces from 8.48 to 7.42 (Fig. 6a, e), from 22.33 to 10.23 (Fig. 6b, f), from 1.43 to zero (Fig. 6c, g), and from 16.17 to 1.96 (Fig. 6d, h). This is attributed to the combined effects of fiber dispersion and frequency chirp, which are induced by the pseudo-random bit pattern effect that increases under high-speed modulation and depends on the history of “0” bits preceding every “1” bit [51]. That is, the influences of α and ϵ on the chirp characteristics increases with lengthening the optical fiber.

Figure 7a, b plots variations of the Q -factor with the fiber length under the investigated two values of the gain suppression coefficient ($\epsilon=0.5 \times 10^{-17}$ and $5 \times 10^{-17} \text{ cm}^3$) when $\alpha=1$ and 10, respectively. The figures confirm the combined effects of the fiber length and frequency chirp on the Q -factor. In more details, as the fiber length and/or α -factor increase, the Q -factor reduces, whereas it is enhanced when

ϵ increases. As mentioned in Sect. 2, according to the ITU-T recommendations, BER is limited by 10^{-12} , which is sufficient for free error transmission and corresponds to Q -factor ≈ 7 . Accordingly when $\alpha=1$, the maximum fiber lengths (L_{\max}) that corresponds to transmission free from error is 2.52 and 5.89 km when $\epsilon=0.5 \times 10^{-17}$ and $5 \times 10^{-17} \text{ cm}^3$, respectively, as shown in Fig. 7a. When $\alpha=10$, L_{\max} reduces to 0.3 and 0.78 km when $\epsilon=0.5 \times 10^{-17}$ and $5 \times 10^{-17} \text{ cm}^3$, respectively, as shown in Fig. 7b. These results confirm that the frequency chirp parameters (α and ϵ) are significant contributors to the fiber length limitation, which agrees with the explanations reported in Ref. [51].

Determining the maximum fiber length L_{\max} basing on the frequency chirp parameters (α and ϵ) is an important issue in the design of high-speed optical fiber links. To provide a more detailed picture, Fig. 8 plots the predicted values of L_{\max} in terms of the α -factor and ϵ . The figure reveals that L_{\max}

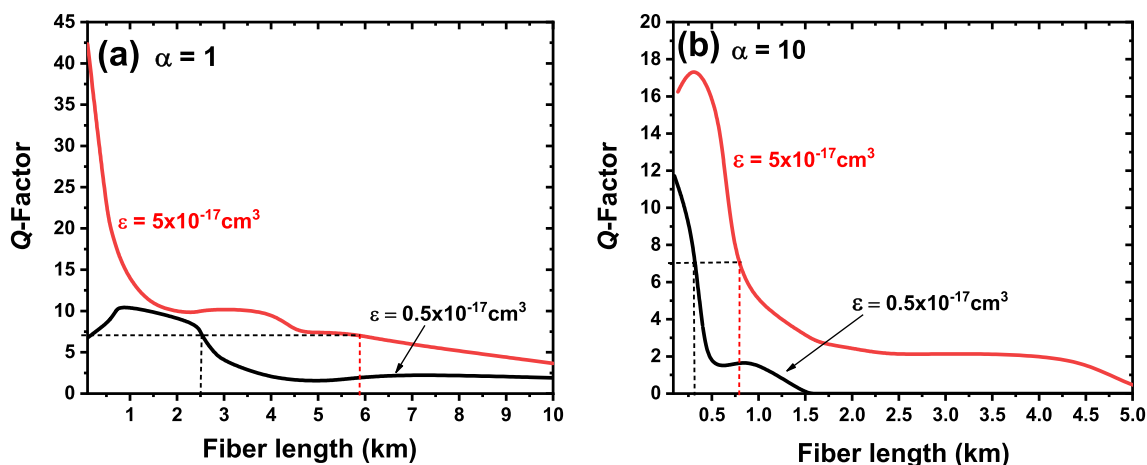


Fig. 7 Q -factor versus fiber length at small gain suppression coefficient ϵ of $0.5 \times 10^{-17} \text{ cm}^3$ (black line), and at large coefficient ϵ of $5 \times 10^{-17} \text{ cm}^3$ (red line) when **a** $\alpha = 1$, and **b** $\alpha = 10$

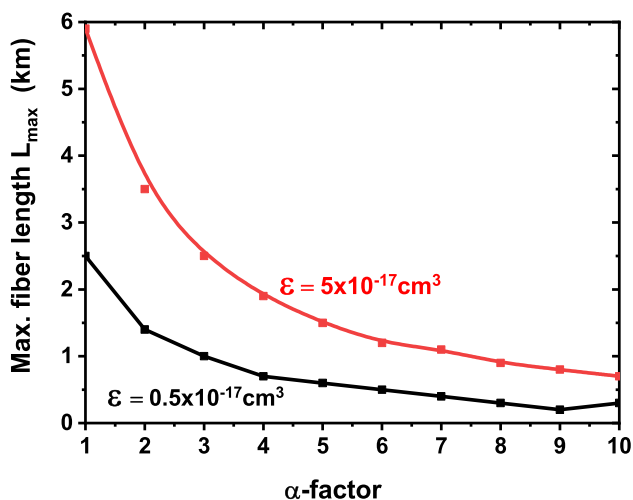


Fig. 8 Maximum fiber length L_{max} versus α -factor at small ϵ of $0.5 \times 10^{-17} \text{ cm}^3$ (black line), and at large ϵ of $5 \times 10^{-17} \text{ cm}^3$ (red line)

decreases with the increase of α -factor and/or decrease in ϵ . In other words, one should reduce α -factor and increase the gain suppression coefficient ϵ to increase the maximum transmission distance. As a numerical example, when α increases from 1 to 10, L_{max} decreases from 5.89 to 0.78 km at large $\epsilon = 5 \times 10^{-17} \text{ cm}^3$, and decreases from 2.52 to 0.3 km at small $\epsilon = 0.5 \times 10^{-17} \text{ cm}^3$, respectively. These results, to the best of the authors' knowledge, are new contributions to dependence of the upper limit of the transmission distances on α and ϵ .

4 Conclusion

This paper introduced a numerical simulation study on the chirping characteristics of a direct modulated high-speed 1.55 μm laser diode and assessed its performance for use

in 40 Gbps optical fiber links. The effects of the linewidth enhancement factor α and the gain suppression coefficient ϵ on the chirp characteristics and fiber transmission length were investigated. The chirp characteristics included the modulated signal waveform, frequency peak-to-peak chirp, and laser output wavelength spectrum. The performance of 40 Gbps optical fiber link was evaluated in terms of the eye diagram and the Q -factor and the maximum fiber length. The results show that when α increases from 1 to 10, the modulated laser waveform exhibits pronounced relaxation oscillations in both the "1" or "0" bits with strong peak overshoots, which results in a sharp increase in the laser peak-to-peak chirp from 21.8 to 205 GHz when $\epsilon = 0.5 \times 10^{-17} \text{ cm}^3$ due to contribution of the transient chirp. The increase of ϵ to $5 \times 10^{-17} \text{ cm}^3$ increase the difference between the "1" and "0" levels, which induces an adiabatic chirp and dampens out the peak overshoots and reduces the transient chirp and the peak-to-peak chirp from 19.5 to 193.3 GHz. However, the increase of ϵ causes significant shifts in the lasing wavelength $\Delta\lambda$ relative to the actual non-modulated laser wavelength and degrades the efficiency of the laser diode in WDM applications due to the channel interference. These obtained results, to the best of the authors' knowledge, are new contributions to dependence of the lasing wavelength shift on α and ϵ in 40-Gbps WDM systems. However, the increase of ϵ induces an increase in the degree of eye-opening and the Q -factor, which enhances performance of the fiber link. In contrast, the increase of the α -factor increases the eye-closure and reduces the Q -factor, which degrades performance of the fiber link. As the fiber length increases, the influences of α and ϵ on the chirp characteristics become more significant. The predicted maximum fiber length L_{max} decreases with the increase in α and/or decrease in ϵ ; when α increases from 1 to 10, L_{max} decreases from 5.89 to 0.78 km at $\epsilon = 5 \times 10^{-17} \text{ cm}^3$, and decreases from 2.52 to 0.3 km when

$\varepsilon = 0.5 \times 10^{-17} \text{ cm}^3$. The obtained results are new contributions to variations of the maximum transmission distances with α and ε .

Acknowledgements We thank Prof. Moustafa Ahmed, Department of Physics, Faculty of Science, King Abdulaziz University for offering help in revising the manuscript.

Funding Open access funding provided by The Science, Technology & Innovation Funding Authority (STDF) in cooperation with The Egyptian Knowledge Bank (EKB). This research did not receive any specific grant from funding agencies in the public, commercial, or not-for-profit sectors.

Declarations

Conflict of interest The authors declare no conflicts of interest.

Open Access This article is licensed under a Creative Commons Attribution 4.0 International License, which permits use, sharing, adaptation, distribution and reproduction in any medium or format, as long as you give appropriate credit to the original author(s) and the source, provide a link to the Creative Commons licence, and indicate if changes were made. The images or other third party material in this article are included in the article's Creative Commons licence, unless indicated otherwise in a credit line to the material. If material is not included in the article's Creative Commons licence and your intended use is not permitted by statutory regulation or exceeds the permitted use, you will need to obtain permission directly from the copyright holder. To view a copy of this licence, visit <http://creativecommons.org/licenses/by/4.0/>.

References

- ITU-T draft recommendation G. 693, Optical Interfaces for Intra-Office Systems, ITU-T Study Group 15 (2001-2004), approved under the WSA Resolution 1 procedure on 29 Nov. 2001
- G.P. Agrawal, *Optical Fiber Communication Systems* (Van Nostrand Reinhold, New York, 2003)
- B. Dagens, A. Martinez, D. Make, O. Le Gouezigou, J.G. Provost, V. Sallet, B. Thedrez, Floor free 10-gb/s transmission with directly modulated gain-as-gaas 1.35- μm laser for metropolitan applications. *IEEE Photon. Technol. Lett.* **17**(5), 971–973 (2005)
- C. Henry, Phase noise in semiconductor lasers. *J. Lightwave Technol.* **4**(3), 298–311 (1986)
- G.P. Agrawal, N.K. Dutta, *Long wavelength semiconductor lasers*, vol. 1 (Van Nostrand Reinhold, New York, 1986)
- K. Sato, S. Kuwahara, Y. Miyamoto, Chirp characteristics of 40-Gb/s directly modulated distributed-feedback laser diodes. *J. Lightwave Technol.* **23**(11), 3790 (2005)
- M.F. Ahmed, A.H. Bakry, F.T. Albelady, Digital modulation characteristics of high-speed semiconductor laser for use in optical communication systems. *Arab. J. Sci. Eng.* **39**(7), 5745–5752 (2014)
- S. Yamamoto, M. Kuwazuru, H. Wakabayashi, Y. Iwamoto, Analysis of chirp power penalty in 1.55- μm DFB-LD high-speed optical fiber transmission systems. *J. Lightwave Technol.* **5**(10), 1518–1524 (1987)
- B.W. Hakki, Evaluation of transmission characteristics of chirped DFB lasers in dispersive optical fiber. *J. Lightwave Technol.* **10**(7), 964–970 (1992)
- C. del Río Campos, P.R. Horche, A.M. Minguez, Interaction of semiconductor laser chirp with fiber dispersion: Impact on WDM directly modulated system performance, in *Proceedings of The Fourth International Conference on Advances in Circuits, Electronics and Micro-electronics, CENICS* (2011), pp. 17–22
- R.S. Tucker, High-speed modulation of semiconductor lasers. *IEEE Trans. Electron Devices.* **32**(12), 2527 (1985)
- P. Krehlik, Directly modulated lasers in negative dispersion fiber links. *Opto-Electron. Rev.* **15**(2), 71–77 (2007)
- M. Ahmed, Modeling and simulation of dispersion-limited fiber communication systems employing directly modulated laser diodes. *Indian J. Phys.* **86**(11), 1013–1020 (2012)
- C. del Río Campos, P.R. Horche, Directly modulated laser intrinsic parameters optimization for WDM Systems, in *2008 International Conference on Advances in Electronics and Micro-electronics* (IEEE, 2008), pp. 78–83
- M. Ahmed, S.W. Mahmoud, A.A. Mahmoud, Influence of pseudorandom bit format on the direct modulation performance of semiconductor lasers. *Pramana* **79**(6), 1443–1456 (2012)
- G. Arnold, P. Russer, Modulation behavior of semiconductor injection lasers. *Appl. Phys.* **14**(3), 255–268 (1977)
- C. Henry, Theory of the linewidth of semiconductor lasers. *IEEE J. Quantum Electron.* **18**(2), 259–264 (1982)
- M. Osinski, J. Buus, Linewidth broadening factor in semiconductor lasers-An overview. *IEEE J. Quantum Electron.* **23**(1), 9–29 (1987)
- T.L. Koch, R.A. Linke, Effect of nonlinear gain reduction on semiconductor laser wavelength chirping. *Appl. Phys. Lett.* **48**(10), 613–615 (1986)
- A. Hangauer, G. Wysocki, Gain compression and linewidth enhancement factor in mid-IR quantum cascade lasers. *IEEE J. Sel. Top. Quantum Electron.* **21**(6), 74–84 (2015)
- G. Wang, R. Nagarajan, D. Tauber, J. Bowers, Reduction of damping in high-speed semiconductor lasers. *IEEE Photonics Technol. Lett.* **5**(6), 642–645 (1993)
- C. del Río Campos, P.R. Horche, *Effects of Dispersion Fiber on CWDM Directly Modulated System Performance* (IntechOpen, New York, 2012), pp. 55–76
- K. Vahala, L.C. Chiu, S. Margalit, A. Yariv, On the linewidth enhancement factor α in semiconductor injection lasers. *Appl. Phys. Lett.* **42**(8), 631–633 (1983)
- G.P. Agrawal, N.K. Dutta, *Semiconductor Lasers*, 2nd edn. (Van Nostrand Reinhold, New York, 1993)
- R.A. Abdullah, The influence of gain suppression on dynamic characteristics of violet InGaN laser diodes. *Optik* **125**(1), 580–582 (2014)
- M. Ahmed, M. Yamada, An infinite order perturbation approach to gain calculation in injection semiconductor lasers. *J. Appl. Phys.* **84**(6), 3004–3015 (1998)
- M.J. Adams, M. Osinski, Influence of spectral hole-burning on quaternary laser transients. *Electron. Lett.* **19**(16), 627–628 (1983)
- J.E. Bowers, T.L. Koch, B.R. Hemenway, D.P. Wilt, T.J. Bridges, E.G. Burkhardt, High-frequency modulation of 1.52 μm vapour-phase-transported InGaAsP lasers. *Electron. Lett.* **21**(7), 297–299 (1985)
- K. Furuya, Y. Suematsu, T. Hong, Reduction of resonancelike peak in direct modulation due to carrier diffusion in injection laser. *Appl. Opt.* **17**(12), 1949–1952 (1978)
- B.N. Gomati, A.P. DeFonzo, Gain suppression in semiconductor lasers: the influence of dynamic carrier temperature changes. *J. Appl. Phys.* **64**(3), 1555–1557 (1988)
- A. Yousuf, Investigation on chirping characteristics of a 1.55- μm directly modulated distributed feedback laser. *J. Opt.* **47**(4), 481–488 (2018)

32. A. Yousuf, Effect of gain compression above and below threshold on the chirp characteristics of 1.55 μm distributed feedback laser. *Opt. Rev.* **23**(6), 897–906 (2016)
33. S.W. Mahmoud, Influence of gain suppression on static and dynamic characteristics of laser diodes under digital modulation. *Egypt J. Solids* **30**, 237–251 (2007)
34. Z.B.A. Mutalip, Frequency chirp characteristics on WDM direct modulation, in *2010 Second International Conference on Computer Engineering and Applications*, Vol. 1 (IEEE, 2010), pp. 125–128
35. F.T. Albeladi, M.F. Ahmed, A.H. Bakry, Performance evaluation of 40 Gb/s directly-modulated optical fiber communication systems, in *2013 Saudi International Electronics, Communications and Photonics Conference* (IEEE, 2013), pp. 1–6
36. E. Peral, W.K. Marshall, A. Yariv, Precise measurement of semiconductor laser chirp using effect of propagation in dispersive fiber and application to simulation of transmission through fiber gratings. *J. Lightwave Technol.* **16**(10), 1874–1880 (1998)
37. C. del Río Campos, P.R. Horche, A. Martín-Minguez, Analysis of linewidth and extinction ratio in directly modulated lasers for performance optimization in 10 Gbit/s CWDM systems. *Opt. Commun.* **283**(15), 3058–3066 (2010)
38. J.C. Cartledge, G.S. Burley, The effect of laser chirping on lightwave system performance. *J. Lightwave Technol.* **7**(3), 568–573 (1989)
39. R. Nagarajan, M. Ishikawa, T. Fukushima, R.S. Geels, J.E. Bowers, High speed quantum-well lasers and carrier transport effects. *IEEE J. Quantum Electron.* **28**(10), 1990–2008 (1992)
40. M. Yamada, Y. Suematsu, Analysis of gain suppression in undoped injection lasers. *J. Appl. Phys.* **52**(4), 2653–2664 (1981)
41. A. Tomita, A. Suzuki, A new density matrix theory for semiconductor lasers, including non-Markovian intraband relaxation and its application to nonlinear gain. *IEEE J. Quantum Electron.* **27**(6), 1630–1641 (1991)
42. R. Al-Otaibi, M. Ahmed, Modelling of intensity noise, frequency noise and linewidth of semiconductor laser and their dependence on optical gain formulation. *Pramana* **95**(3), 1–11 (2021)
43. I. Tomkos, I. Roudas, R. Hesse, N. Antoniadis, A. Boskovic, R. Vodhanel, Extraction of laser rate equations parameters for representative simulations of metropolitan-area transmission systems and networks. *Opt. Commun.* **194**(1–3), 109–129 (2001)
44. T.L. Koch, J.E. Bowers, Nature of wavelength chirping in directly modulated semiconductor lasers. *Electron. Lett.* **20**(25), 1038–1040 (1984)
45. G.P. Agrawal, *Chapter 2: Optical Fibers. Fiber-Optic Communication Systems* (Wiley, New York, 1997)
46. A. Mahmoud, M. Ahmed, Generation of frequency comb and its dependence on gain suppression in directly modulated semiconductor laser. *Appl. Phys. B* **127**(8), 1–11 (2021)
47. M. Ahmed, A. El-Lafi, Analysis of small-signal intensity modulation of semiconductor lasers taking account of gain suppression. *Pramana* **71**(1), 99–115 (2008)
48. B. Zhao, T.R. Chen, A. Yariv, The gain and carrier density in semiconductor lasers under steady-state and transient conditions. *IEEE J. Quantum Electron.* **28**(6), 1479–1486 (1992)
49. A. Villafranca, J. Lasobras, I. Garcés, Precise characterization of the frequency chirp in directly modulated DFB lasers, in *2007 Spanish Conference on Electron Devices* (IEEE, 2007), pp. 173–176
50. F. Kariminezhad, E. Rajaei, A. Fali, R. Mirzaei, Impact of gain compression factor on modulation characteristics of InGaAs/GaAs self-assembled quantum dot lasers. *J. Theor. Appl. Phys.* **10**(4), 281–287 (2016)
51. M. Ahmed, Effect of fiber attenuation and dispersion on the transmission distance of 40-Gb/s optical fiber communication systems using high-speed lasers. *Phys. Wave Phenom.* **22**(4), 266–272 (2014)

Publisher's Note Springer Nature remains neutral with regard to jurisdictional claims in published maps and institutional affiliations.